Modeling and Position Control of the HASEL Actuator via Port-Hamiltonian Approach

Yu Yeh, Nelson Eduardo Cisneros Pinto, Yongxin Wu, Kanty Rabenorosoa,
Yann Le Gorrec

Modeling and Position Control of the HASEL Actuator via port-Hamiltonian Approach

Yu Yeh, Nelson Cisneros, Yongxin Wu, Kanty Rabenorosoa, Yann Le Gorrec

Abstract—**This paper deals with the modeling and control problem of a Hydraulically Amplified Self-healing Electrostatic (HASEL) actuator based on the port-Hamiltonian framework. A nonlinear spring-damper system is used to approximate the mechanical deformation of the actuator due to the motion of the fluid while a nonlinear capacitance is used to approximate the electric behavior of the system. The actuator position control strategy is investigated based on the Interconnection Damping Assignment-Passivity Based Control (IDA-PBC) method, with further Integral Actions (IA) added to cope with load uncertainties. The proposed model and control laws are validated on an experimental benchmark. The experimental tests demonstrate that the proposed model is accurate up to 94% of fitness. The controllers allow assigning the actuator position with ramp and sinusoidal references with the relative error less than 5%. At last, the robustness of the proposed IDA-PBC controller with IA has been shown with the experimental result for the unknown load disturbance rejection.**

Index Terms—**Soft robot, soft actuator, HASEL actuator, port-Hamiltonian approach, IDA-PBC method**

I. INTRODUCTION

Robots based on soft actuators have drawn more and more attention of the researchers during the last decade due to their safety for humans and suitability to unknown environments. Recent studies have shown that robots based on soft actuators perform competitively with existing solid robots in terms of force and strain [1]. Soft pneumatic actuators and dielectric elastomer actuators are two popular kind of soft actuators. In the recent years, the Hydraulically Amplified Self-Healing Electrostatic (HASEL) actuator has provided a new road-map for the design of soft actuators [2]. By combining the design concept of dielectric elastomer actuators and pneumatic soft actuators, more desirable features of HASEL actuators are indicated [3] including self-sensing and self-healing capabilities and great potential for many applications, such as: HASEL artificial muscles made from elastomers, elastomeric donuts, quadrant donuts and curling HASEL actuators [4], soft grippers [2] and soft-actuated joints created based on the hydraulic mechanism used in spider legs [5]. One of the advantages of the HASEL actuator is that it is easy to manufacture, low cost, and open to many potential design based on its working principle [6]. The authors of [7] present an easy to implement toolkit to design and fabricate multiple HASEL

actuators incorporating electrostatic zipping mechanisms and reducing operating voltages. Several attempts to model and control the HASEL actuator have recently been proposed. In [8], the geometrical analysis of HASEL is investigated. In [9], an identification of a nonlinear HASEL actuator model has been presented and the controller design using the self-sensing strain is addressed with a basic control approach. In [10], the planar HASEL actuator model is investigated to describe the relationship between the output force and the applied voltage. These works reveal that the modeling and control of complex mechanical structure with fluid structure interaction is very hard and challenging. Only few studies on control-oriented modeling and control design has been proposed in the literature [9].

To overcome these constraints, this paper proposes a physically based dynamic model and a control strategy for HASEL actuators using the port-Hamiltonian (PH) approach. This approach [11] has proven to be powerful for the modeling and control of complex multi-physical systems [12], [13]. PH modeling is based on the characterization of energy exchanges between the different components of the system. This approach is particularly adapted for the modular modeling of multi-physical systems. On the other hand, the PH approach is well suited passivity based control design with clear physical interpretation, such as energy shaping and control by interconnection and damping assignment (IDA-PBC) [14]. The PH approach and IDA-PBC control method have been investigated for the modeling and control of a flexible beam using the Ionic Polymer Metal Composite (IPMC) actuators in [15]. In this work, the flexible beam has been considered under small deformation and modeled by a linear infinite dimensional system and a very simple RC circuit model has been considered for the IPMC actuator. The overall system is then governed by a linear coupled Partial Differential Equation (PDE) – Ordinary Differential Equation (ODE) model. The control method has been proposed for the discretized model without any investigation on the robustness of the controller.

A common design of HASEL actuators consists in clustering HASEL units as shown in the right figure of Fig 1, and each unit consists of pouches filled with dielectric fluid and covered with pairs of electrodes. The pouch is formed by flexible but inextensible polymer films made bonding shell. While the voltage is applied, the corresponding Maxwell force zips the paired electrodes and displaces the dielectric liquid. Because of the inextensible properties of the polymer films and dielectric liquid, the displacement of liquid causes the deformation of the pouches, leading to the motion of endpoints of the actuator.

Fig. 1: Experimental setup description

Fig. 2: (a) The geometry of HASEL unit; (b) Deformation description of the actuator
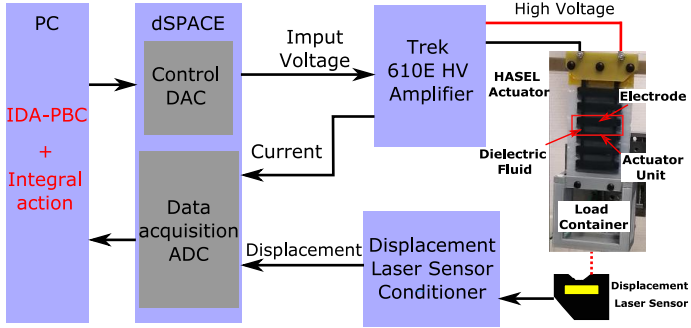
The main contributions of this paper are the proposition of a PH model to describe the dynamics of the HASEL actuator and the position control strategy based on the IDA-PBC method. The geometry of the HASEL pouch is investigated and based on this analysis, a PH dynamic model is established using a non linear spring-damper system to approximate the mechanical behavior of the flowing liquid in the pouches. Different from to the work presented in [15], a precise model is proposed considering both the electrical and mechanical parts of the actuator, leading to a non linear finite dimensional model in this paper. A control law based on IDA-PBC method is employed to achieve the desired equilibrium position. An integral action is added to the previous controller to cope with the uncertainties in the load mass which has not been considered in [15]. The proposed PH model is identified and validated by an experimental setup and the proposed control method is also validated by the same experimental setup which is described in Fig. 1.

This paper is organized as follow: Section II presents the geometry analysis and the PH modeling of the HASEL actuator. The IDA-PBC based position control and integral action are proposed in Section III. In Section IV, the experimental setup and the parameters identification are presented. The proposed control laws is experimentally validated and the results are discussed in Section V. Some final remarks and future works are given in Section VI.

II. PORT HAMILTONIAN MODELING OF HASEL ACTUATOR

In the following sections, the geometric constraints of the system are introduced. All the geometric variables can be interpreted as function of the endpoint displacement q (the geometry of HASEL actuator is shown in Fig 2b), the partial derivative of these variables are naturally derived and which is essential for the PH model.

A. Geometry description of HASEL actuator

We first introduce the HASEL unit, which is a simplified geometric model to approximate the real actuator. Unlike an ellipse geometric shape presented in [4], we use a diamond shape to describe the unit pouch of the HASEL actuator as shown in Fig. 2a.

The HASEL unit is composed of a pouches filled with dielectric liquid, and equiped with a pair of electrodes covering the two polymer films. The parameters of the actuator include:
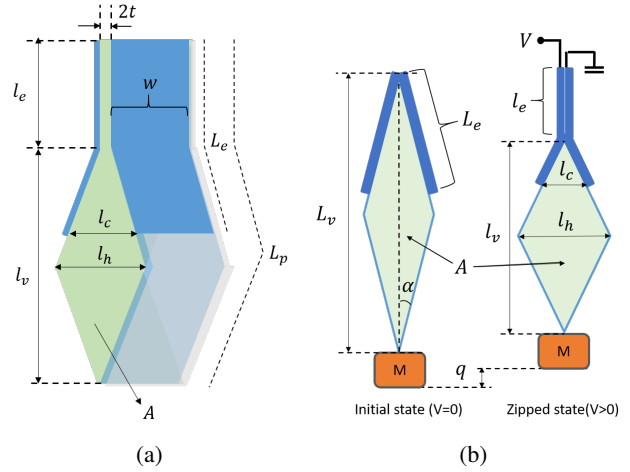
- L_p the length of pouches;
- w the width of pouches and electrodes;
- L_e the length of paired electrodes;
- L_v the initial length of actuator;
- A the cross-sectional area of pouches;
- t the thickness of dielectric film.

When we apply the voltage to the actuator, the Maxwell force zips the pair of electrodes which leads to the deformation of actuator. We define the geometric variables due to the deformation as follows:

- l_e the length of the zipped electrodes;
- l_h the height of the pouches;
- l_v the length of the unzipped pouches;
- l_c the distance between the endpoints of the paired electrodes.

In this paper, we make two assumptions for the actuator during its deformation: 1) the cross-section area A is constant because the dielectric liquid is incompressible, and 2) the length of the pouch L_p is constant because the membrane is inextensible. The objective is to find how the displacement q relates to the geometry of the HASEL unit. From the deformation of the actuator, we can write the geometrical relationship to achieve the different variables. The actuator endpoint displacement is defined as:

$$q = L_v - (l_e + l_v) = \Omega(l_e) \tag{1}$$

Since the cross-sectional area is assigned to a diamond shape, the following geometry relationship holds:

$$A = \frac{l_v l_h}{2}$$
$$(L_p - l_e)^2 = l_v^2 + l_h^2 \tag{2}$$

By substituting the first equation of (2) to the second one, we can present the height l_h and the width l_v as the function of l_e as following:

$$l_h = \sqrt{\frac{(L_p - l_e)^2}{2} - \sqrt{\frac{(L_p - l_e)^4}{4} - 4A^2}} \tag{3}$$

$$l_v = \sqrt{\frac{(L_p - l_e)^2}{2} + \sqrt{\frac{(L_p - l_e)^4}{4} - 4A^2}} \qquad (4)$$

Then we can substitute the above equation to Eq. (1) and the length of the zipped electrodes l_e can be presented as a function of the actuator endpoint displacement q:

$$l_e(q) = \Omega^{-1}(q) \qquad (5)$$

Finally, the geometric constraints of the actuator can written as a function of the displacement q.

The more precise geometric analysis of the actuator has been made based on the ellipse shape in [8], [16]. In this paper we have chosen the the diamond shape for the dynamic modeling, because it is a good compromise between the accuracy of the model and its simplicity of the geometric analysis. All the geometric variables can be expressed in the function of q with the diamond shape assumption. However, in the ellipse shape case, it is not easy to present or compute all the geometric variables in the function of q.

B. PH Formulation of HASEL

In this part, we derive a dynamic model of the HASEL actuator by using the PH framework. The main idea is the use of spring damper systems to describe the mechanical properties of the dielectric liquid in pouch. The motivation is from the observation of the physical properties during the actuator deformation: 1) the displacement of the liquid and the constraints on the structure cause the resistance to the deformation, and 2) the actuator returns to its initial state (position) when the voltage is switched off. These properties imply that the mechanical properties of the flowing dielectric liquid can be described by a spring-damper system. In this paper, we propose two spring-damper systems places in the vertical and horizontal directions of the actuator, as shown in Fig. 3.
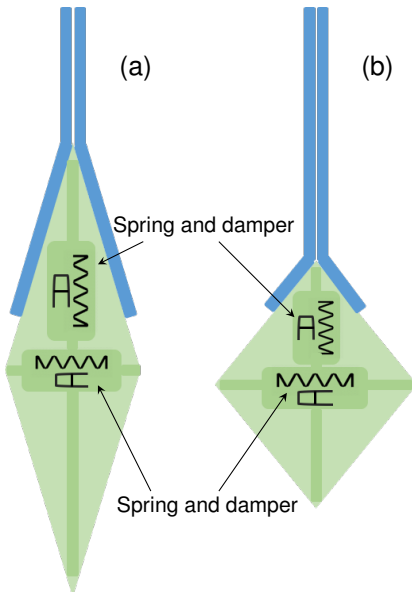

Fig. 3: (a) Initial state when load is placed at the end; (b) The deformed state with zipped part of electrodes.

To model the dynamics of the actuator, we first introduce its Hamiltonian function (energy function) which is composed by the mechanical energy and the electric energy. The total mechanical energy is the sum of the kinetic and the potential energy. The potential energy of the spring system is written as

$$H_s(q) = \frac{1}{2}k_v(q)\Delta\xi_v(q)^2 + \frac{1}{2}k_h(q)\Delta\xi_h(q)^2 \qquad (6)$$

where $\Delta\xi_v(q)$, $\Delta\xi_h(q)$ are the deformation of the springs in the vertical and horizontal directions, and $k_v(q)$, $k_h(q)$ are the coefficients of the nonlinear springs. The deformation of the springs are defined as

$$\begin{aligned}\Delta\xi_v(q) = l_v(q) - \xi_v(m)\\ \Delta\xi_h(q) = l_h(q) - \xi_h(m)\end{aligned} \qquad (7)$$

where ξ_v, ξ_h are the original length of the springs. In this work, the original length of the springs are designed as nonlinear functions depending on the load mass m. Because the geometry constrains limit initial states of the actuator, no matter how heavy the load is applied to the actuator, the initial states should remain the same. From a physical point of view, it can be explained by the fact that the uncompressible dielectric liquid generates an equivalent inner pressure to resist to the external force from the load and maintains the actuator in the initial geometry.

The electric energy of the capacitance between the paired electrodes is

$$H_c(q,Q) = \frac{1}{2}\frac{Q^2}{C(q)} \qquad (8)$$

where Q is the charge of the capacitor and C is the capacitance value. While C depends on q, its computation can be split into two parts: the zipped region and unzipped region. The capacitance in the zipped region can be described by

$$C_z(q) = \frac{\epsilon_r\epsilon_0 w}{2t}l_e(q) \qquad (9)$$

For the unzipped region, it is approximated by the capacitance between two unparalleled plates

$$C_{uz}(q) = \int_0^{(L_e - l_e)\cos(\alpha)} \frac{\epsilon_r\epsilon_0 w\tan(\alpha)}{2t + 2x\tan(\alpha)}dx \qquad (10)$$

As a result, the total capacitance is

$$C(q) = C_z(q) + C_{uz}(q) \qquad (11)$$

Then including the kinetic energy of the load and the potential energy related to the gravity, the Hamiltonian function, *i.e.* the total energy of the system can be described as:

$$H(q,p,Q) = H_s(q) + H_c(q,Q) + \frac{1}{2}\frac{p^2}{m} + mgq \qquad (12)$$

where the p is the momentum of the load and g is the gravity constant. By choosing the energy variables as the state variables $x = [q, p, Q]^T$. The co-energy variables e are:

$$e = \begin{bmatrix}\frac{\partial H}{\partial q}\\\frac{\partial H}{\partial p}\\\frac{\partial H}{\partial Q}\end{bmatrix} = \begin{bmatrix}\frac{\partial H_c}{\partial q} + \frac{\partial H_s}{\partial q} + mg\\\frac{p}{m}\\\frac{Q}{C(q)}\end{bmatrix} \qquad (13)$$

where $\frac{\partial H}{\partial q}$ stands for the total force working on the load in the q direction, resulting from the sum of the spring force working on the load $\frac{\partial H_s}{\partial q}$, the force from capacitance $\frac{\partial H_s}{\partial q}$ and the gravity force mg.

With the above variables, the dynamics of the actuator can be presented by the following PH formulation:

$$\begin{bmatrix} \dot{q} \\ \dot{p} \\ \dot{Q} \end{bmatrix} = \underbrace{\begin{bmatrix} 0 & 1 & 0 \\ -1 & -b(q) & 0 \\ 0 & 0 & -1/r \end{bmatrix}}_{(J-R)} \begin{bmatrix} \frac{\partial H}{\partial q} \\ \frac{\partial H}{\partial p} \\ \frac{\partial H}{\partial Q} \end{bmatrix} + \underbrace{\begin{bmatrix} 0 \\ 0 \\ 1/r \end{bmatrix}}_{g} V \quad (14)$$

where the interconnection matrix $J = -J^T$ represents the energy exchanges in the system, while the damping matrix $R = R^T = \mathrm{diag}\begin{bmatrix} 0 & b(q) & 1/r \end{bmatrix} \geq 0$ describes the internal dissipation of the system with $b(q)$ the nonlinear damping coefficient depending on the vertical and horizontal damper and r the resistance of the actuator. Let choose the current, the power conjugate variable of the input, as the output $y = g^T \frac{\partial H}{\partial x} = i$, the system is passive, since the Hamiltonian is such that $H > 0$ and $H(0) = 0$, moreover its time derivative satisfies:

$$\dot{H} = -\frac{\partial H}{\partial x}^T R \frac{\partial H}{\partial x} + y^T u \leq y^T u. \quad (15)$$

III. POSITION CONTROL DESIGN

In this work, the objective is to control the end position of the HASEL in closed loop. Based on the PH model proposed in the previous section, the IDA-PBC method will be investigated to control the position of the actuator. The IDA-PBC method provides several degrees of freedom to assign the closed-loop equilibrium position and performance with clear physical interpretation from energy point of view [14]. Furthermore, a structure preserving integral action will be added to improve the robustness of the control law while guaranteeing the closed-loop stability.

A. Basics of IDA-PBC Design

For the design procedure of the IDA-PBC method, let consider the open loop system (14):

$$\dot{x} = (J - R)\frac{\partial H}{\partial x} + g(x)u. \quad (16)$$

Define an asymptotically stable PH target system

$$\dot{x} = (J_d - R_d)\frac{\partial H_d}{\partial x} \quad (17)$$

where the matrices $J_d(x) = -J_d(x)^T$, $R_d(x) = R_d^T(x) \geq 0$ and the function H_d that satisfy the following matching equation:

$$g^\perp (J_d - R_d)\frac{\partial H_d}{\partial x} = g^\perp (J_d - R_d)\frac{\partial H}{\partial x} \quad (18)$$

with $g^\perp$ a full rank left annihilator of g, i.e $g^\perp g = 0$. $H_d(x)$ is the desired Hamiltonian (closed-loop energy) function such that $x^* = \arg\min H_d(x)$, with x^* the equilibrium to be stabilized. The closed-loop system (17) with the feedback law $u = \beta(x)$, where

$$\beta(x) = (g^T g)^{-1} g^T ((J_d - R_d)\frac{\partial H_d}{\partial x} - (J - R)\frac{\partial H}{\partial x}) \quad (19)$$

behaves as the target system with the equilibrium x^* asymptotically stable.

B. Application to HASEL actuator position control

To apply the IDA-PBC design procedure on the HASEL actuator position control, we firstly consider the open loop system (16) and define the desired closed-loop Hamiltonian function

$$H_d(p,q,Q) = \frac{k_p}{2}(q-q^*)^2 + \frac{1}{2}\frac{p^2}{m} + \frac{k_Q}{2}(Q-Q^*)^2 \quad (20)$$

where q^* and Q^* are the desired equilibrium position and charge of capacitance, and the asymptotically stable PH target system corresponds to (17) with

$$J_d = \begin{bmatrix} 0 & J_{12} & \alpha_1 \\ -J_{12} & 0 & \alpha_2 \\ -\alpha_1 & -\alpha_2 & 0 \end{bmatrix}, R_d = \begin{bmatrix} 0 & 0 & 0 \\ 0 & r_1 & 0 \\ 0 & 0 & \frac{1}{r} \end{bmatrix}$$

where α_1, α_2 are the frees variable to be designed. By defining the full rank left annihilator $g^\perp = \begin{bmatrix} -1 & 0 & 0 \\ 0 & 1 & 0 \end{bmatrix}$, the matching equation (18) leads to

$$J_{12}(q,p,Q) = 1 - \alpha_1 \frac{m}{p}k_Q(Q-Q^*)$$
$$r_1(q,p,Q) = b + \frac{m}{p}(\frac{\partial H}{\partial q} - J_{12}k_p(q-q^*)- \quad (21)$$
$$-\alpha_2 k_Q(Q-Q^*))$$

which are the variable depending on the state variables q,p,Q. The desired equilibrium of the system is $x^* = \begin{bmatrix} q^*, 0, Q^* \end{bmatrix}$. To make sure the closed loop system is asymptotically stable, the parameter $r_1 \geq 0$ which implies

$$Q^* \geq \frac{\alpha_2 k_Q Q - \kappa}{\alpha_2 k_Q} \quad (22)$$

where $\kappa = b + \frac{m}{p}(\frac{\partial H}{\partial q} - J_{12}k_d(q-q^*))$ According to equation (19), the control law of closed-loop system is

$$\beta(x) = -\alpha_1 r k_p(q-q^*) - k_Q(Q-Q^*) + \frac{Q}{C(q)} - \alpha_2 r \frac{p}{m} \quad (23)$$

C. Integral Action (IA) for robustness

The main drawback of the controller proposed in the previous section is the lack of robustness to overcome the steady state error due to the external disturbance or the unmatched mass of load. To improve the robustness, the integral action control [17] based on the IDA-PBC method is applied in this subsection.

The uncertainties of the load can be interpreted as external force applied on the system. Hence, the closed-loop system in the previous section can be expressed as

$$\begin{bmatrix} \dot{Q} \\ \dot{p} \\ \dot{q} \end{bmatrix} = \begin{bmatrix} J_d(x) - R_d(x) \end{bmatrix} \begin{bmatrix} \frac{\partial H}{\partial Q} \\ \frac{\partial H}{\partial p} \\ \frac{\partial H}{\partial q} \end{bmatrix} + \begin{bmatrix} 0 \\ d \\ 0 \end{bmatrix} \quad (24)$$

where the matrices $J_d(x)$ and $R_d(x)$ are defined as

$$J_d(x) := \begin{bmatrix} J_{aa}(x) & J_{au}(x) \\ -J_{au}^T(x) & J_{uu}(x) \end{bmatrix} = \begin{bmatrix} 0 & -\alpha_1 & -\alpha_2 \\ \alpha_1 & 0 & -J_{12} \\ \alpha_2 & J_{12} & 0 \end{bmatrix}$$

$$R_d(x) := \left[\begin{array}{c|c} R_{aa}(x) & R_{au}(x) \\ \hline -R_{au}^T(x) & R_{uu}(x) \end{array}\right] = \left[\begin{array}{c|cc} \frac{1}{r} & 0 & 0 \\ \hline 0 & 0 & 0 \\ 0 & 0 & r_1 \end{array}\right]$$

and d is a unknown constant external force (disturbance) to the system that depends on the unknown load. According to [17], if we choose the new closed-loop Hamiltonian function H_{cl}

$$H_{cl} = H_d + \frac{K_i}{2}\|Q - x_c\|^2, \tag{25}$$

we can derive the new closed-loop Hamiltonian system

$$\left[\begin{array}{c} \dot{x}_a \\ \dot{x}_u \\ \dot{x}_c \end{array}\right] = \left[J_{cl}(x) - R_{cl}(x)\right] \left[\begin{array}{c} \frac{\partial H_{cl}}{\partial x_a} \\ \frac{\partial H_{cl}}{\partial x_u} \\ \frac{\partial H_{cl}}{\partial x_c} \end{array}\right] + \left[\begin{array}{c} 0 \\ d \\ 0 \\ 0 \end{array}\right]. \tag{26}$$

Thus the control law of the integral action is

$$u_i = \left[-J_{aa} + R_{aa} + J_{c_1} - R_{c_1} - R_{c_2}\right]\frac{\partial H_d}{\partial x_a} \tag{27}$$
$$+ \left[J_{c_1} - R_{c_1}\right]K_i(x_a - x_c) + 2R_{au}\frac{\partial H_d}{\partial x_u}$$

$$\dot{x}_c = -R_{c_2}\frac{\partial H_d}{\partial x_a} + (J_{au} + R_{au})\frac{\partial H_d}{\partial x_u} \tag{28}$$

where x_c is the state of integral action. In this paper, we choose the following design of matrices:

$$J_{c_1} = 0, \ R_{c_1} = \frac{1}{r}, \ R_{c_2} = 0 \tag{29}$$

and the interconnection and damping matrices given by

$$J_{cl} := \left[\begin{array}{ccc} 0 & J_{au}(x) + R_{au}(x) & 0 \\ -(J_{au}^T(x) + R_{au}^T(x)) & J_{uu}(x) & 0 \\ 0 & 0 & 0 \end{array}\right]$$

$$R_{cl} := \left[\begin{array}{ccc} 1/r & 0 & 1/r \\ 0 & R_{uu}(x) & 0 \\ 1/r & 0 & 1/r \end{array}\right]. \tag{30}$$

Then the following integral control law and the controller state can be derived:

$$u_i = \frac{1}{r}K_i(Q - x_c) \tag{31}$$

$$\dot{x}_c = -\alpha_1 k_p(q - q^*) - \alpha_2 \frac{p}{m} \tag{32}$$

where K_i is the gain of the integral action need to be designed. Combining the IDA-PBC (23) and Integral action (31), we can implement the controller as the block diagram in Fig. 4.
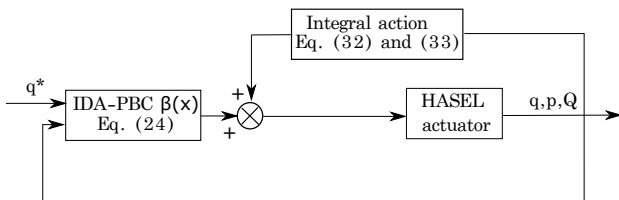

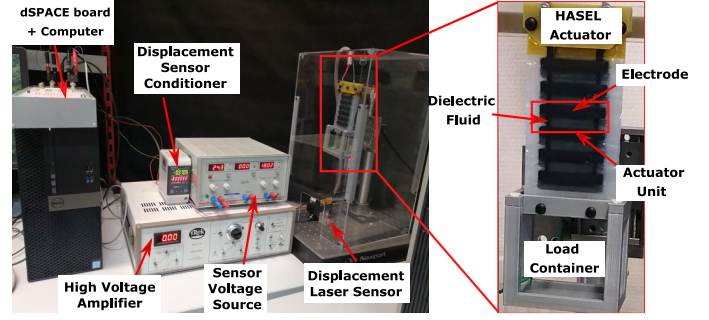Fig. 4: Block diagram of closed-loop control with integral action

Fig. 5: Experimental setup

IV. EXPERIMENT DESCRIPTION AND IDENTIFICATION

A. Experiment Setup

The experimental setup description is presented as shown in Fig. 1 in Introduction . The real-life experimental setup is shown in Fig. 5 and composed of the following elements:

- The actuator used in this study is composed of 5 C-5015 HASEL actuators that were manufactured by $Artimus\ Robotic^®$. A 3-D printed load container is attached to the bottom of the actuator to simplify the load change during the manipulation.
- A $Trek^®610E$ high voltage amplifier is used to linearly amplify $0-10V$ input signal to $0-10KV$ output voltage with guaranteeing the current up to $2mA$ which provides sufficient driven power for the actuator motion. This amplifier can also return the current measurement in real-time during the manipulation.
- A $Kenyence^®$LK-G152 laser sensor is used to measure the actuator displacement. The sensor is tuned to have $10kHz$ of bandwidth and $\pm4cm$ measurement range which are large enough to track the dynamics of the actuator and to validate the proposed control law.
- A computer with $Matlab\ Simulink^®$is used to generate the reference signals, to implement the proposed controller and to get the measurement data.
- A $dSPACE\ board$ ($dS1104$) serves the signals converters interface such as DAC (digital analogic converter) between the computer and the actuator and the ADC (analogic digital converter) between experimental sensor measurement (displacement and current) and the computer.

The HASEL actuator has the self-sensing property for its strain measurement [2] which can be used for the controller implementation. The aim of this paper is to propose an accurate and reliable dynamic model and passivity based position control law for the HASEL actuator. In this case, we use a high precision laser displacement sensor instead of self-sensing measurement to avoid the error which can occur in the self-sensing.

B. Model Identification and Validation

For the model identification and the experimental validation, we conduct experiments with different loads ($m = 150g$, $200g$, $250g$) and different applied voltages ($V = 4kV$, $5kV$, $6kV$)

to obtain the experimental data of the displacement q and the electrical charge Q. The objective of identification is to find the proper coefficients of the spring-damper systems which approximate the dynamics of dielectric liquid of the HASEL actuator. From the system (14), we can obtain the mechanical force of the HASEL actuator as $F_m = \frac{\partial H_s}{\partial q} + F_d = \dot{p} - \frac{\partial H_c}{\partial q} - mg$ with $F_d = b(q)\frac{p}{m}$. Thus the identification problem becomes to find the optimal solution for the original length, the stiffness of the springs and the damper coefficients such that the difference between the mechanical force F_m and the measured force F_e is minimum.

Fig. 6: Mechanical force identification
(Fitness: 94%)

TABLE I: HASEL actuator's parameters

Parameter	Value	Units
L_p	0.012	m
L_e	0.06	m
w	0.05	m
t	18×10^{-6}	m
ϵ_0	8.85×10^{-12}	F/m
ϵ_r	2.2	F/m
r	8000	Ω

The coefficients are nonlinear and defined as the first order polynomial form:

$$\xi_i(m) = \phi_1^j m + \phi_0^j$$
$$k_i(q) = \theta_1^j q + \theta_0^j \qquad (33)$$
$$b_i(q) = \lambda_1^j l_i(q) + \lambda_0^j$$

where $j = v, h$ stands for the vertical and horizontal directions. The length of the springs is the function of the load m with coefficients ϕ_n^j, the stiffness and the damper are the function of deformation with coefficients θ_n^j and λ_n^j. The identification problem is solved by the nonlinear model identification ('*nl-greyest*') and the trust-region-reflective algorithm ('*fmincon*') which are implemented in Matlab Identification Toolbox®.

The experimental data of the mechanical force used for the parameters identification are shown by the blue curve in Fig. 6. Using the identification toolbox as mentioned before, one can get the identified parameters. Then the model simulation result with the identified parameters is compared to the experimental data in Fig. 6. The curve fitting has a very high percentage (fit = 94%) where fit = $\left[100 \left(1 - \frac{\|y_{exp} - y_{sim}\|}{\|y_{exp} - mean(y_{exp})\|} \right) \right] \%$ with the experimental data y_{exp} and the model simulation result y_{sim}.

In order to verify the previous identified parameters, the actuator position response in the simulation is also compared to the experimental position data as shown in Fig. 7 with high fitness (88%). Meanwhile, the model with the identified parameters provides high fitness both in position and force response in the case of the different loads and the different applied voltages. These results suggest that the proposed model is able to describe the dynamics of the HASEL actuator.

V. CONTROL IMPLEMENTATION

In this section, we implement the proposed IDA-PBC controller (23) and the Integrate action (31) to the actuator with identified parameters to get the desired positions. Fig.
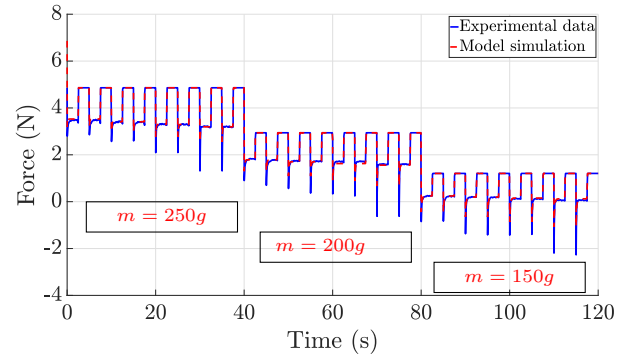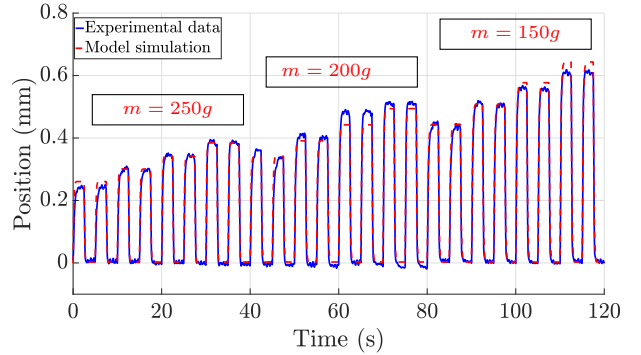

Fig. 7: Position identification
(Fitness: 88%)

8 shows the closed loop responses with IDA-PBC controller with $k_p = 4$, $k_Q = 2$ and $\alpha_2 = 0.1$ (blue dashed line) and IDA-PBC + IA controller with $K_i = 1$ (red solid line) which follow the desired position defined as the successive ramp reference between $[0.5\text{mm}, 3, 5\text{mm}]$ (black dotted line). From Fig. 8, the closed loop responses with and without IA controller both follow the reference in a satisfactory way and the the difference is not easy to see. The relative error ($e_r = \frac{\text{absolute error}}{\text{reference}}$) of the closed-loop responses are 3% to 5% with and without IA controller. In this paper, the controller parameters tuning rules are not investigated. The investigation on PID-PBC controller parameters tuning for a class of linear (linearized) port Hamiltonian mechanical systems can be found [18]. The IDA-PBC controller parameters tuning rules of proposed controllers in this paper shall be investigated in the future.

In Fig 9, we use a sinusoidal reference signal to define the desired position. The signal frequency is 0.2Hz and the signal range is $[0.5\text{mm}, 2\text{mm}]$ (black dotted line). In this case, we only use the IDA-PBC + IA controller to control the actuator. The experimental result shows the closed loop response (red solid line) follows well the reference (upper figure). The maximal error of the signal tracking is around 0.1mm and with 4% relative error.

In Figure 10, we show the effectiveness of the proposed IDA-PBC+IA controller to the frequency position assignment.
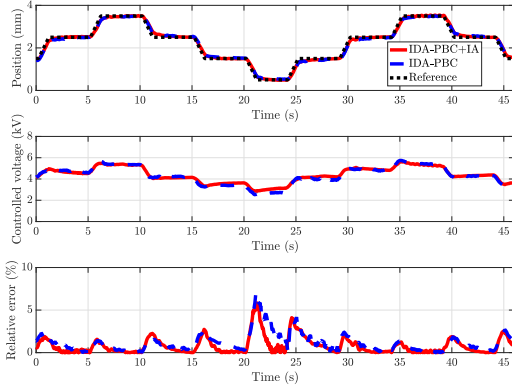
Fig. 8: Position control with the successive ramp reference signal (Upper figure); Control voltage (Middle figure); Relative error e_r (Bottom figure)
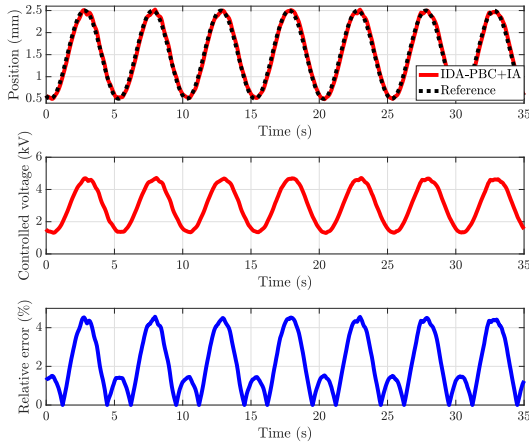

Fig. 9: Position control with the sinusoidal signal (Upper figure); Control voltage (Middle figure); Relative error e_r (Bottom figure)

The desired position is defined by the sinusoidal reference with 1 Hz, 3 Hz, 5 Hz, 7 Hz. We can see the proposed controller can guarantee the position assignment with different frequencies.

From Fig. 8, one can observe that the IA does not significantly improve the closed loop performance. But as mentioned before, the purpose of using IA is to improve the robustness of the controller to the unknown load disturbance. In Fig. 11, we show the robustness improvement with the IA (red solid line) compared to the IDA-PBC controller without IA (blue dotted line). We assign the desired position to 2mm and 0.5mm. A 100g load mass is added in the load container when the actuator position at 2mm and removed when the position at 0.5mm. we can see that the closed loop position is disturbed when we add or remove the load mass for both controllers. The IDA-PBC can not reject this external disturbance while the closed loop response with IDA-PBC+IA controller goes back to the desired position as expected.
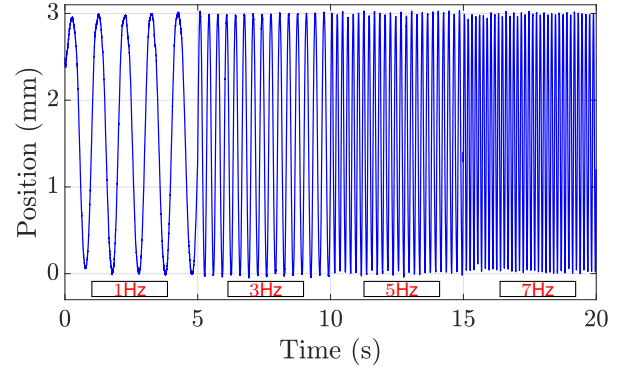

Fig. 10: Position responses of the sinusoidal signal with 1 Hz, 3 Hz, 5 Hz, 7 Hz, respectively.)
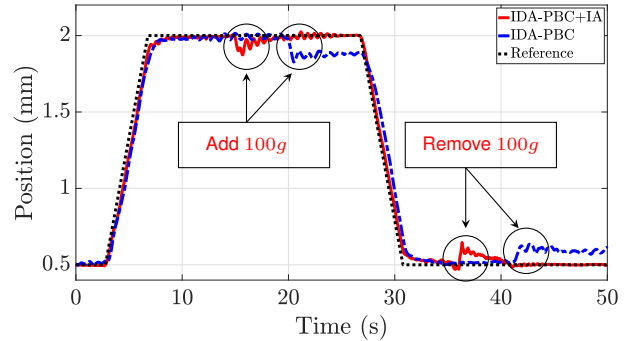

Fig. 11: Disturbance rejection with Integral Action on the IDA-PBC controller

VI. CONCLUSION

In this work, we propose a dynamic model of an HASEL actuator via the port-Hamiltonian approach. The mechanical behavior of the actuator is approximated by two perpendicular nonlinear spring-damper systems. The proposed model reproduces the main dynamic behavior of the actuator. The experimental results show that the proposed model is sufficiently accurate to cope with the main system dynamics (up to 94% fitness). Based on the proposed model, the IDA-PBC method is investigated for the positioning control of the actuator. Further integral action is added to cope with load uncertainties. The experimental closed loop responses validate the proposed control laws to different desired position references with the relative error less than 5%. This work is the first attempt to the control-oriented modeling and control design of the HASEL actuator taking the advantage of the PH approach. In the future, the dynamic modeling and control design for more complex structures based on the HASEL actuator will be investigated. The high speed position control design and the controller parameters tuning problem will be considered in the future.

REFERENCES

[1] D. Rus and M. Tolley, "Design, fabrication and control of soft robots," *Nature*, vol. 521, pp. 467–75, 05 2015.

[2] E. Acome, S. K. Mitchell, T. G. Morrissey, M. B. Emmett, C. Benjamin, M. King, M. Radakovitz, and C. Keplinger, "Hydraulically amplified self-healing electrostatic actuators with muscle-like performance," *Science*, vol. 359, no. 6371, pp. 61–65, 2018.

[3] P. Rothemund, N. Kellaris, S. K. Mitchell, E. Acome, and C. Keplinger, "Hasel artificial muscles for a new generation of lifelike robots-recent progress and future opportunities." *Advanced materials*, 2020.

[4] P. Rothemund, S. Kirkman, and C. Keplinger, "Dynamics of electrohydraulic soft actuators," *Proceedings of the National Academy of Sciences*, vol. 117, no. 28, pp. 16 207–16 213, 2020.

[5] N. Kellaris, P. Rothemund, Y. Zeng, S. K. Mitchell, G. M. Smith, K. Jayaram, and C. Keplinger, "Spider-inspired electrohydraulic actuators for fast, soft-actuated joints," *Advanced Science*, vol. 8, no. 14, p. 2100916, 2021.

[6] N. Kellaris, V. Gopaluni Venkata, G. M. Smith, S. K. Mitchell, and C. Keplinger, "Peano-hasel actuators: Muscle-mimetic, electrohydraulic transducers that linearly contract on activation," *Science Robotics*, vol. 3, no. 14, 2018.

[7] S. K. Mitchell, X. Wang, E. Acome, T. Martin, K. Ly, N. Kellaris, V. G. Venkata, and C. Keplinger, "An easy-to-implement toolkit to create versatile and high-performance hasel actuators for untethered soft robots," *Advanced Science*, vol. 6, no. 14, p. 1900178, 2019.

[8] N. Kellaris, V. G. Venkata, P. Rothemund, and C. Keplinger, "An analytical model for the design of peano-hasel actuators with drastically improved performance," *Extreme Mechanics Letters*, vol. 29, p. 100449, 2019.

[9] B. K. Johnson, V. Sundaram, M. Naris, E. Acome, K. Ly, N. Correll, C. Keplinger, J. S. Humbert, and M. E. Rentschler, "Identification and control of a nonlinear soft actuator and sensor system," *IEEE Robotics and Automation Letters*, vol. 5, no. 3, pp. 3783–3790, 2020.

[10] D.-X. Liu, J. Bao, D. Liu, Y. Lu, and J. Xu, "Modeling of planar hydraulically amplified self-healing electrostatic actuators," *IEEE Robotics and Automation Letters*, vol. 6, no. 4, pp. 7533–7540, 2021.

[11] B. Maschke and A. van der Schaft, "Port-controlled Hamiltonian systems: Modelling origins and systemtheoretic properties," *IFAC Proceedings Volumes*, vol. 25, no. 13, pp. 359–365, 1992, 2nd IFAC Symposium on Nonlinear Control Systems Design 1992, Bordeaux, France, 24-26 June.

[12] V. Duindam, A. Macchelli, S. Stramigioli, and H. Bruyninckx, *Modeling and Control of Complex Physical Systems: The Port-Hamiltonian Approach*. Springer Publishing Company, Incorporated, 2014.

[13] A. Dòria-Cerezo, C. Batlle, and G. Espinosa-Pérez, "Passivity-based control of a wound-rotor synchronous motor," *Control Theory & Applications, IET*, vol. 4, pp. 2049 – 2057, 11 2010.

[14] R. Ortega, A. van der Schaft, B. Maschke, and G. Escobar, "Interconnection and damping assignment passivity-based control of port-controlled Hamiltonian systems," *Automatica*, vol. 38, no. 4, pp. 585–596, 2002.

[15] W. Zhou, Y. Wu, H. Hu, Y. Li, and Y. Wang, "Port-Hamiltonian modeling and IDA-PBC control of an IPMC-actuated flexible beam," *Actuators*, vol. 10, no. 9, 2021.

[16] G. Moretti, M. Duranti, M. Righi, R. Vertechy, and M. Fontana, "Analysis of dielectric fluid transducers," in *Electroactive Polymer Actuators and Devices (EAPAD) XX*, Y. Bar-Cohen, Ed., vol. 10594, International Society for Optics and Photonics. SPIE, 2018, pp. 142 – 154.

[17] J. Ferguson, A. Donaire, R. Ortega, and R. H. Middleton, "New results on disturbance rejection for energy-shaping controlled port-Hamiltonian systems," *arXiv*, 2017. [Online]. Available: https://arxiv.org/abs/1710.06070

[18] C. Chan-Zheng, P. Borja, and J. M. A. Scherpen, "Tuning rules for a class of passivity-based controllers for mechanical systems," *IEEE Control Systems Letters*, vol. 5, no. 6, pp. 1892–1897, 2021.